universe

MDPI

Article

Collisions of Electrons with Alkali, Alkaline and Complex Atoms Relevant to Solar and Stellar Atmospheres

Moncef Derouich [1,*], Saleh Qutub [1], Fainana Mustajab [2] and Badruddin Zaheer Ahmad [1]

[1] Astronomy and Space Science Department, Faculty of Science, King Abdulaziz University, P.O. Box 80203, Jeddah 21589, Saudi Arabia
[2] Physics Deparment, University Polytechnic, Jamia Millia Islamia, New Delhi 110025, India
* Correspondence: aldarwish@kau.edu.sa

Abstract: In solar and stellar atmospheres, atomic excitation by impact with electrons plays an important role in the formation of spectral lines. We make use of available experimental and theoretical cross-sections to calculate the excitation rates in s–p transitions of alkali and alkaline atoms through collisions with electrons. Then, we infer a general formula for calculating the excitation rates by using genetic programming numerical methods. We propose an extension of our approach to deduce collisional excitation rates for complex atoms and atoms with hyperfine structure. Furthermore, the developed method is also applied to determine collisional polarization transfer rates. Our results are not specific to a given atom and can be applied to any s–p atomic transition. The accuracy of our results is discussed.

Keywords: collisions; solar energy; Sun: atmosphere; stars: atmospheres; atomic data; light formation

check for updates

Citation: Derouich, M.; Qutub, S.; Mustajab, F.; Ahmad, B.Z. Collisions of Electrons with Alkali, Alkaline and Complex Atoms Relevant to Solar and Stellar Atmospheres. *Universe* **2022**, *8*, 613. https://doi.org/10.3390/universe8120613

Academic Editor: Viorel-Puiu Paun

Received: 12 October 2022
Accepted: 14 November 2022
Published: 23 November 2022

Publisher's Note: MDPI stays neutral with regard to jurisdictional claims in published maps and institutional affiliations.

Copyright: © 2022 by the authors. Licensee MDPI, Basel, Switzerland. This article is an open access article distributed under the terms and conditions of the Creative Commons Attribution (CC BY) license (https://creativecommons.org/licenses/by/4.0/).

1. Statement of the Problem

One of the most important areas in collision physics is the study of inelastic electronic excitation of atoms by impact with free electrons. In fact, accurate evaluation of atom–electron collision rates plays a fundamental role in the analysis of astrophysical spectra. By considering these rates in spectroscopic and spectropolarimetric models, several important new phenomena in solar and stellar physics have been revealed (e.g., [1–7]).

Ref. [8] established theoretical formula for electron-impact-excitation cross-sections based on the unitless Gaunt factor g, which is applicable for allowed dipole transitions. This formula was put to practical use by [9] who analyzed the experimental and theoretical data known at that time to infer an effective empirical Gaunt factor $\overline{g}$, which is commonly called the g-bar-factor. As of its simplicity, the $\overline{g}$ semi-empirical van Regemorter formula has been the most widely employed approach for about 60 years, when no specific quantum calculations or experimental measurements are available. It is often interesting to make approximations to obtain general and compact formulae allowing manageable and efficient calculations of collisional rates for astrophysical applications.

In this context, the g-bar formula provided by Seaton–van Regemorter's pioneer works is widely employed. In fact, during the last 5 years, the paper was cited more than 100 times for astrophysical applications. This situation needs to be improved in the sense that new easily applicable but more accurate collisional approaches must be determined in order to keep abreast of the observational advances brought by modern instrumentation. Present astrophysical observations permit the precise analysis of the physical conditions of the regions where the spectral lines form, provided that one understands the underlying collision physics.

Our work is focused on the determination of the collisional rates for excitation of alkali and alkaline atoms by electrons. Based on up-to-date genetic programming (GP) numerical methods (e.g., [10–12] for details), we use the obtained rates to infer a compact formula allowing collisional rate calculation for all s–p transitions of simple atoms. Let us recall that GP

is inspired from the evolution theory of Darwin. It is a numerical technique allowing, through an evolutionary algorithm, the gradual optimization of a population of formula to increase their degree of adaptation to perform a fitting and to solve complex problems (e.g., [12,13]).

We show how to determine the collisional rates for atoms with a hyperfine structure and complex atoms. We find that our results for simple and complex atoms are in agreement with quantum models with confirmed accuracy and with experimental data. This work is a continuation of our aim to provide general collisional data for astrophysical applications (see [12]).

2. Available Experimental and Theoretical Data for Simple Atoms

We start by collecting available trustable data corresponding to cross-sections obtained for simple atoms in collisions with electrons. As will be shown later in this paper, the collisional rates for complex atoms and atoms with hyperfine structure can be derived from the collisional rates for simple atoms through linear combinations. The simple atoms considered in the present paper are defined as atoms with only one valence electron in a p-state above a filled sub-shell or above an electron in an s-state (e.g., [14]).

In fact, electron-impact-excitation cross-sections were measured experimentally for nine alkali and alkaline simple atoms: Mg, Ca, Sr, Ba, Li, Na, K, Rb and Cs ([15–21]). Table 1 collects the references, electronic configurations for s–p transitions and threshold energies ΔE for the nine simple atoms. Values of ΔE are available in the literature and can be found, for example, in the NIST database.

Table 1. s–p excitations of nine simple atoms. Values of ΔE are available in the NIST database.

Experimental Reference	s–p Atomic Transition	Threshold Energy ΔE (eV)
[21]	Cs ($5\,p^6\,6s\,^2S$ <—> $5\,p^6\,6p\,^2P$)	1.4546
[21]	Rb ($4\,p^6\,5s\,^2S$ <—> $4\,p^6\,5p\,^2P$)	1.5890
[21]	K ($3\,p^6\,4s\,^2S$ <—> $3\,p^6\,4p\,^2P$)	1.6171
[18]	Li ($1\,s^2\,2s\,^2S$ <—> $1\,s^2\,2p\,^2P$)	1.8478
[16]	Na ($2\,p^6\,3s\,^2S$ <—> $2\,p^6\,3p\,^2P$)	2.1044
[20]	Ba ($5\,p^6\,6\,s^2\,^1S$ <—> $5\,p^6\,6\,s\,6p\,^1P$)	2.2391
[19]	Sr ($4\,p^6\,5\,s^2\,^1S$ <—> $4\,p^6\,5\,s\,5p\,^1P$)	2.6902
[17]	Ca ($3\,p^6\,4\,s^2\,^1S$ <—> $3\,p^6\,4\,s\,4p\,^1P$)	2.9324
[21]	Mg ($2\,p^6\,3\,s^2\,^1S$ <—> $2\,p^6\,3\,s\,3p\,^1P$)	4.3457

Theoretical works have succeeded and have been mainly concerned with the case of Na, which is one of the most studied atoms (e.g., [22–25]). As can be seen in Figures 1 and 2, experimental results in the case of Na ([16]) agree well with theoretical quantum models of [22–24]. Theoretical works, such as [23], confirm the experimental results for the {Na + e} collisions with kinetic energies smaller than 5 eV. [25] agrees with the experimental results of [16] even at high energies of 10^4 eV or larger (see Figure 1). We also verified that the quantum results of [26] concerned with {Li + e} collisions agree well with the experimental results of [18].

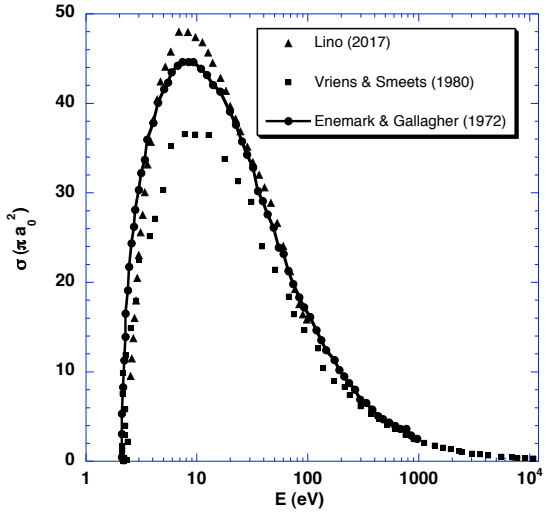

Figure 1. Excitation cross-sections σ_{lu} (in $\pi\, a_0^2$) of the {Na-e} collisions as a function of the kinetic energies E(eV) up to 10^4 eV. [15,22,25].

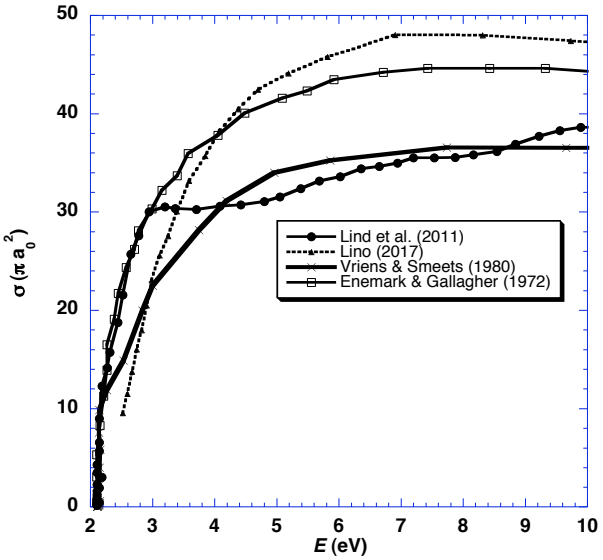

Figure 2. Excitation cross-sections σ_{lu} ($\pi\, a_0^2$) of the {Na-e} collisions as a function of small kinetic energies E(eV) up to 5 eV. [15,22,24,25].

Gallagher and collaborators used similar experimental set ups to obtain results for all simple atoms between 1972 and 1978 (see Table 1). Since Gallagher et al.'s experiments are in good agreement with the recent theoretical works for {Na + e} and {Li + e} collisions (e.g., [24–26]), one can assume that their experimental results for other simple atoms are sufficiently precise. This encourages us to use all of these available experimental data (see Table 1) as well as theoretical data to derive our formulation.

Experimental results were obtained for all energy regimes, from 0 to 10^5 eV, which allows us to determine the collisional rates for a wide range of temperatures needed for solar and stellar diagnostics.

3. Fitting Formula Inferred for Simple Atoms

The kinetic energies E of the electrons impacting target atoms should be larger than the threshold energy ΔE to induce excitation. For $E < \Delta E$, excitation is not possible. Subthreshold excitations are out of the scope of our work. If one denotes the s-lower

level by (l) and the p-upper level by (u), the collisional excitation rate C_{lu} is given by the following expression:

$$C_{lu}(T) = N_e \sqrt{\frac{8}{\pi\mu(k_B T)^3}} \int_{\Delta E}^{\infty} E\, \sigma_{lu}(E)\, \exp(\frac{-E}{k_B T})\, dE, \quad (1)$$

Note that the excitation cross-section $\sigma_{lu}(E)$ is zero for energies $E < \Delta E$. In addition, μ is the reduced mass of the system, which is practically equal to the electron mass, where N_e is the electron density, T is the temperature, and k_B is the Boltzmann constant. The de-excitation collisional rate is:

$$C_{ul} = \frac{w_l}{w_u} C_{lu}\, \exp(\frac{\Delta E}{k_B T}), \quad (2)$$

where w_u and w_l are the statistical weights of the upper level (u) and the lower level (l).

We use Equations (1) and (2) to calculate the excitation and de-excitation collisional rates of the alkali and alkaline atoms Mg, Ca, Sr, Ba, Li, Na, K, Rb and Cs for temperatures going from 500 to 20,000 K. These rates are obtained through averaging the experimental cross-sections of A. Gallagher's group over a Maxwellian distribution of velocities (or kinetic energies) [15–21]. We find that the excitation rates C_{lu} can be clearly small for temperatures $T < 2000$ K and, in general, C_{lu} have a complicated dependence on T. However, the de-excitation rates C_{ul} are characterized by a smoother dependence on T. Furthermore, C_{lu} and C_{ul} depend strongly on the threshold energy ΔE.

Since the C_{lu} and C_{ul} are related by Equation (2), it is sufficient to compute C_{ul} to obtain C_{lu} and vice versa. C_{ul} can be given as a function of ΔE for a given temperature, and it is a function of T for a specific value of ΔE. For ΔE = 1.4546 eV (Cs atom) and 4.3457 eV (Mg atom), the variation laws with T are:

$$\begin{aligned} C_{ul}(\Delta E = 1.4546) &= 2.909 \times 10^{-8}\ T^{0.25031}\ (\mathrm{cm^3\ s^{-1}}) \\ C_{ul}(\Delta E = 4.3457) &= 2.796 \times 10^{-9}\ T^{0.3318}\ (\mathrm{cm^3\ s^{-1}}) \end{aligned} \quad (3)$$

with the correlation factors R = 0.99804 and R = 0.98724, respectively.

Equation (3) gives the C_{ul} rate as a function of one variable, which is T, and thus it is applicable only for specific atomic transitions characterized by its threshold energy ΔE. In general, the C_{lu} and C_{ul} rates are functions of two variables, ΔE and T.

One must perform a generalized fit to obtain two-variable functions giving C_{lu} and C_{ul} for any values of ΔE and T. As mentioned previously, it is more convenient to fit the de-excitation rates C_{ul} since their dependence on T is smoother than the dependence of C_{lu} on T. We apply sophisticated methods based on GP in order to fit all the available experimental results for a wide range of temperatures and for all ΔE values. As a result, in Equation (4), we provide simple atom de-excitation rates $[C_{ul}]_{\mathrm{GP}}$ as a function of the (ΔE, T) parameters for temperatures ranging from 500 to 20,000 K. By using the notations $z = [C_{ul}]_{\mathrm{GP}}$ (in $\mathrm{cm^3\ s^{-1}}$), $x = \Delta E$ (in eV) and $y = T$ (in K), we obtain the following highly non-linear relationship:

$$\begin{aligned} z = {} & 1.16994 \times 10^{-8} [0.367879 \times (-7. + x) \\ & + \exp(-x) \times y^{0.5} - \frac{21. \times (-3. + x) \times \sin(x)}{(3. + x)}] \end{aligned} \quad (4)$$

Equation (4) is the core result of the present work since it allows, in a compact and efficient way, general calculations of collisional rates for all simple atoms. In addition, as will be seen in the next sections, by using Equation (4), one can calculate the collisional rates for complex atoms and atoms with a hyperfine structure.

In addition, since polarization profiles are currently of great interest, we show how Equation (4) allows the calculation of all polarization transfer rates between *s*- and *p*-levels. Equation (4) was inferred from experimental data.

4. Accuracy of the Application of Our Approach to Simple Atoms

The accuracy of Equation (4) can be evaluated by comparing the $[C_{ul}]_{\mathrm{GP}} = z$ values (called output) to the $[C_{ul}]_{experiment}$ values (called input), which are calculated directly by averaging the experimental cross-sections over the kinetic energies. Comparisons of $[C_{ul}]_{\mathrm{GP}} = z$ with the $[C_{ul}]_{experiment}$ values are given in Table 2 for all simple atom s–p transitions at $T = 5000$ K. In the case of the strong solar line 4227 Å corresponding to the Ca s–p transition, $[C_{ul}]_{experiment} = 3.01 \times 10^{-8}$ cm^3 s^{-1} and $[C_{ul}]_{\mathrm{GP}} = 2.714 \times 10^{-8}$ cm^3 s^{-1}. Thus, the relative error in this case is less than 10%.

Figure 3 shows the perfect theoretical correspondence (output = input) with a solid line together with the fit results, which are presented by squares and circles. The fit results for different temperature ranges are given with different colors for information about the quality of the fitting as a function of the temperature. The averaged relative error is found to be about 10% to 20%, which is sufficiently acceptable for astrophysical applications. It is also important to notice that, in some cases, the relative error can be clearly larger than 20% but the result is still acceptable and can be used as a good indication on the role of the collisions in cases of the absence of more precise rates.

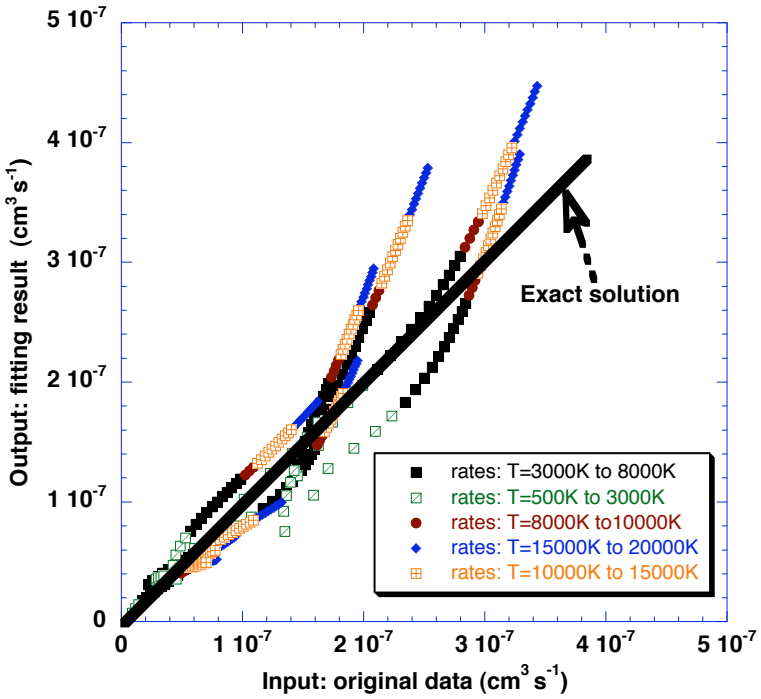

Figure 3. Comparison of the output ($[C_{ul}]_{\mathrm{GP}} = z$) values to the exact rates ($[C_{ul}]_{experiment}$) (called input) calculated directly by averaging the available cross-sections over the kinetic energies. The solid line shows the exact solution and the result of the fit is shown with differently colored squares and circles (as explained in the figure).

For the interesting Sr 4607 Å solar line, the de-excitation rate at $T = 5000$ K, obtained by averaging the experimental cross-section given in [18], is $[C_{ul}]_{experiment} = 3.88 \times 10^{-8}$ cm^3 s^{-1}, which is different by about 10% from the value of $[C_{ul}]_{\mathrm{GP}}$ given by our Equation (4) (see Table 2). On the other hand, the Sr 4607 Å line de-excitation rate can be obtained by using the [9] formulae at $T = 5000$ K where

$$C_{ul;\text{van Regemorter}} = 20.6\ \lambda^3\ T^{-0.5} A_{ul}\ P(\Delta E/k_B T)\ (\lambda \text{ is taken in cm}).$$

We note that the [8] and van [9] formulae neglect close coupling processes, which implies that the collisional transitions obey the same strong selection rules imposed by the radiative processes. This is why $C_{ul;\text{van Regemorter}}$ is proportional to the Einstein coefficient for spontaneous emission A_{ul}. For the case of the Sr 4607 Å line, A_{ul} = 2.01 × 10^8 s^{-1}, ΔE = 2.6902 eV and $P(\Delta E/k_B T) = 0.03465$ (see Table 2 of van Regemorter 1962 [4]). Thus,

$$C_{ul;\text{van Regemorter}} = 1.98 \times 10^{-7} \text{cm}^3\ \text{s}^{-1} \simeq 5 \times [C_{ul}]_{experiment} \quad (5)$$

As established here in Equation (5), the [9] formula is well-known to overestimate excitation cross-sections (see [27]). This overestimation of the collisional rates impacts the modeling and interpretation of astrophysical observations. Equation (4) is an improvement of the van Regemorter g-bar-formula and other classical and semi-classical approaches that are commonly used to model collisions with electrons.

Table 2. s–p de-excitation rates of nine simple atoms obtained for T = 5000 K by using Equation (4) and by directly averaging experimental cross-sections via Equations (1) and (2).

Simple Atom	Threshold Energy ΔE (eV)	$[C_{ul}]_{GP}$ (10^{-7} cm^3 s^{-1}) (Equation (4))	$[C_{ul}]_{experiment}$ (10^{-7} cm^3 s^{-1}) (Direct Calculation)
Cs	1.4546	2.5395	2.4727
Rb	1.5890	2.2111	2.6191
K	1.6171	2.1453	1.8627
Li	1.8478	1.6436	1.5711
Na	2.1044	1.1690	1.4102
Ba	2.2391	0.9566	0.7497
Sr	2.6902	0.4343	0.3876
Ca	2.9324	0.2714	0.3010
Mg	4.3457	0.4132	0.4397

5. Extension to Complex Atoms

5.1. The Frozen Core Approximation

Lines of complex atoms, such as O I, Ti I and Fe I are important in studying solar and stellar atmospheres. In this section, we will extend the results obtained for simple atoms to obtain the rates of collisions of complex atoms with electrons. Atomic energy levels (or spectral terms) are usually denoted by $^{2S+1}L_J$ where L is the orbital quantum number, S is the total spin of the electrons of the complex atom, and J is the total momentum. Our model considers that a complex atom is composed of three parts (see [14,28]):

- Part 1: Electrons in a complete subshell or an electron in an s-state above electrons in a complete subshell.
- Part 2: A partially filled (incomplete) subshell located above part 1, which we call the atom core. L_c and S_c are the total orbital angular momentum of the electrons of the atom core and their total spin, respectively. $^{2S_c+1}L_c$ is the spectral term of the atom core.
- Part 3: A valence/optical electron within an s- or p-state.

In the case of simple atoms, part 2 does not exist, i.e., $S_c = L_c = 0$. We follow L–S coupling schemes to evaluate the collisional rates of complex atoms through simple atom data:

$$\vec{J} = \vec{L} + \vec{S}$$
$$\vec{L} = \vec{L_c} + \vec{l}$$
$$\vec{S} = \vec{S_c} + \vec{s},$$

where l and s are the total orbital momentum and the spin of one valence electron, respectively. As explained in detail by [14], one assumes that only the valence electron is involved in transitions between different levels during the collision—this assumption is

commonly called the frozen core approximation where the core of the complex atom is not sensitive to collisional effects, and then L_c and S_c are conserved during the collision.

In the framework of the frozen core approximation applied here, simple atom data are sufficient to constitute the main core of data, which can be generalized to other kinds of atoms with more complicated structures. We show that the excitation rates $C(J \to J')$ between the $|lSLJ\rangle$ and $|l'SL'J'\rangle$ levels of complex atoms are proportional to $C(l \to l')$:

$$C(J \to J') = (2J'+1)\left(\frac{2L'+1}{2l'+1}\right) C(l \to l') \sum_{k_L} (2k_L+1)\ (-1)^{2S+J+J'+L+L'+L+L'+l'+k_L} \times \begin{Bmatrix} L & L' & l' \\ L' & L & k_L \end{Bmatrix} \begin{Bmatrix} L & S & J \\ S & L & k_L \end{Bmatrix} \begin{Bmatrix} L' & S & J' \\ S & L' & k_L \end{Bmatrix} \quad (6)$$

with $C(l \to l') = C_{lu}$.

By using one summation rule property of the 6-j symbols, we find that:

$$C(J \to J') = (2J'+1)\left(\frac{2L'+1}{2l'+1}\right) C_{lu} \begin{Bmatrix} J & J' & l' \\ L' & L & S \end{Bmatrix}^2 \quad (7)$$

By applying Equations (4) and (7) and by considering that ΔE in Equation (4) is the excitation threshold of the complex atom under study, one can obtain the excitation rate $C(J \to J')$ for any complex atom through impact with electrons. Note that each value of ΔE corresponds to a hypothetical simple atom composed of parts 1 and 3, where $S_c = L_c = 0$. In this sense, C_{lu} plays the role of the excitation rate of a hypothetical simple atom with a threshold energy equal to the energy difference between the upper and lower levels of the studied transition of the complex atom. The excitation rates given in Equation (7) are expressed using the same reasoning and coupling schemes as in [28,29].

5.2. Accuracy of the Rates of Complex Atoms

To confirm the usefulness and accuracy of our approach in the case of complex atoms, we compare our rates to those obtained by [30] for the case of the collisions of the oxygen (which is a complex atom) with electrons. Ref. [30] used a sophisticated R-matrix quantum method to obtain excitation cross-sections as a function of the energy. We averaged these cross-sections to obtain the rates denoted here by $[C_{ul}]_{Rmatrix}$ for two permitted transitions T1 ($2s^2\ 2p^3\ (^4S)\ 3s\ ^3S$ <—> $2s^2\ 2p^3\ (^4S)\ 3p\ ^3P$) and T2 ($2s^2\ 2p^3\ (^4S)\ 3s\ ^5S$ <—> $2s^2\ 2p^3\ (^4S)\ 3p\ ^5P$).

In fact, cross-sections were given by [30] for T1 and T2 transitions between ^{2S+1}L terms, i.e., without considering the J-numbers. Thus, we cannot directly compare our $C(J \to J')$ rates obtained for transitions between $^{2S+1}L_J$ terms with the $[C_{ul}]_{Rmatrix}$ since they are J-independent. To obtain an idea of the accuracy of our approach, we compared the rate $[C_{ul}]_{Rmatrix}$ to C_{ul} of Equation (4).

The C_{ul} corresponds to a hypothetical simple atom having a ΔE equal to the energy difference between the upper and lower levels of the T1 and T2 of the oxygen. This should give us a good indication of the precision of our formula when compared to quantum results. The comparison is not directly suitable since we compare the $[C_{ul}]_{Rmatrix}$ to the corresponding hypothetical simple atom C_{ul}.

As can be seen in Table 3, the largest relative difference between our rates and the R-matrix rates is 48.8%. This difference comes partly from the fact that an accurate/proper comparison is not possible technically. The R-matrix rates available in the literature are defined differently from our rates, which includes an expected difference.

In fact, our intention from this comparison is to make a qualitative comparison to obtain an indication about the accuracy of our Equation (4). However, in any case, the comparison shows that our rates are two-times smaller than the R-matrix rates. On the other hand, the van Regemorter rates are five to ten times larger than the R-matrix rates (see [2]).

Table 3. De-excitation rates obtained for T1 and T2 transitions of the oxygen by collisions with electrons. The rates $[C_{ul}]_{\mathrm{GP}}$ are calculated via Equation (4), and $[C_{ul}]_{Rmatrix}$ are obtained by directly averaging R-matrix quantum cross-sections via Equations (1) and (2). The rates are expressed in $(10^{-7}\mathrm{cm}^3\ \mathrm{s}^{-1})$.

Transition	ΔE (eV)	T(K)	$[C_{ul}]_{Rmatrix}$	$[C_{ul}]_{\mathrm{GP}}$
T1	1.46743	5000	3.93	2.51
	1.46743	7000	4.48	2.86
T2	1.59413	5000	4.25	2.20
	1.59413	7000	4.90	2.51

5.3. Polarization Transfer Rates of Complex Atoms

Next, we concentrate on the polarization transfer rates $D^k(J \to J')$ obtained in the tensorial basis and fundamental for spectro-polarimetric studies where k is the tensorial order. Full details about the $D^k(J \to J')$ and the use of the tensorial basis for polarization studies can be found in the papers by [1,10–12,14,28,29,31–35].

As explained, for example by [28], based on the frozen core approximation, one can show that polarization transfer rates $D^k(J \to J', T)$ between J and J' levels of complex atoms are given by:

$$\begin{aligned} D^k(J \to J') &= (2J+1)(2J'+1)\sum_{k_L}(2k_L+1)D^{k_L}(L \to L')\sum_{k_S}(2k_S+1) \\ &\times \left\{ \begin{array}{ccc} L & S & J \\ L & S & J \\ k_L & k_S & k \end{array} \right\} \left\{ \begin{array}{ccc} L' & S & J' \\ L' & S & J' \\ k_L & k_S & k \end{array} \right\} \end{aligned} \tag{8}$$

where

$$\begin{aligned} D^{k_L}(L \to L') &= (2L+1)(2L'+1)\sum_{k_l}(2k_l+1)D^{k_l}(l \to l')\sum_{k_{L_c}}(2k_{L_c}+1) \\ &\times \left\{ \begin{array}{ccc} l & L_c & L \\ l & L_c & L \\ k_l & k_{L_c} & k_L \end{array} \right\} \left\{ \begin{array}{ccc} l' & L_c & L' \\ l' & L_c & L' \\ k_l & k_{L_c} & k_L \end{array} \right\}, \end{aligned} \tag{9}$$

which becomes, in the case of s–p transition where $l = k_l = 0$:

$$D^{k_L}(L \to L') = \frac{2L'+1}{2l'+1} C_{lu} \sum_{k_L}(-1)^{L+L'+l'+k_L} \left\{ \begin{array}{ccc} L & L' & l' \\ L' & L & k_L \end{array} \right\} \tag{10}$$

The curly brackets are 6-j and 9-j symbols whose numerical calculations are straightforward via some packages, such as in Mathematica. In particular, in case of simple atoms where one has the necessary $L = l = 0$, $L' = l' = 1$ and $k_L = k_l = 0$, one finds, from Equation (10), a typical relationship between the population transfer rates $D^0(l \to l')$ and the excitation rates C_{lu}:

$$D^{k_L}(L \to L') = D^{k_l}(l \to l') = D^0(l \to l') = \sqrt{\frac{2l+1}{2l'+1}}\, C(l \to l') = \frac{1}{\sqrt{2l'+1}} C_{lu} \tag{11}$$

The notations used in the above equations have the same meanings as given in [14,28,29]. In particular, L_c is the angular momentum of the electrons of an incomplete (open) sub-shell, which constitutes the core of the complex atom. More details about the extension to complex atoms can be found in [11,14,28,29].

By combining Equations (8) to (11), one can remark that $D^k(J \to J')$ is given as a function of the C_{ul} provided by the general Equation (4). This is a fundamental result that can be used for spectro-polarimetric applications.

As an example, we consider the particular case of Ti I, which is a complex atom with one interesting 4512.7 Å line that corresponds to the transition between the $3d^3\ (^4F)\ 4s\ (^5F_4)$ and $3d^3\ (^4F)\ 4p\ (^5F_5)$ levels. For the lower level $3d^3\ (^4F)\ 4s\ (^5F_4)$, we have $L_c = 3$, $S_c = 3/2$, $L = 3$, $S = 2$, $J = 4$, $l = 0$, $s = 1/2$, and, for the upper level $3d^3\ (^4F)\ 4p\ (^5F_5)$, we have $L_c = 3$, $S_c = 3/2$, $L' = 3$, $S = 2$, $J' = 5$, $l' = 1$, $s = 1/2$. Once these quantum numbers are introduced in Equations (8) to (11), one obtains all polarization transfer rates for the Ti I levels.

In addition, by taking $k = 0$ in Equation (8), one obtains the excitation collisional rate for the Ti I 4512.7 Å line. Our paper concerns only cases of complex atom transitions with valence electrons in $l = 0$ and $l' = 1$ since the available data are associated only with s–p transitions. It would be highly desirable in the future to extend the results of this paper to p-d and d-f transitions but this depends on the availability of simple atom data. It is useful to mention that the method developed in the present work can be adopted for any l and l' values.

Equations (8) and (9) are a generalization of Equation (7) for $k > 0$. One can recover Equation (7) giving the $C(J \to J')$ rates by simply using Equations (8) and (9) for the particular cases where $k = 0$ and $l = k_l = 0$ since (e.g., [31]):

$$C(J \to J') = \sqrt{\frac{2J'+1}{2J+1}}\, D^{k=0}(J \to J') \tag{12}$$

As $D^k(J \to J')$ and C_{ul} are related, the implementation of the effect of the collisions in the numerical codes associated with the resolution of the statistical equilibrium Equations (SEE) becomes easier for simple/complex atoms. Let us recall that Equations (8) and (9), established for complex atoms, permit recovering the expression of rates of simple atoms by taking $L_c = 0$. For example, through Equation (9), one can verify that $D^{k_L}(L \to L') = D^{k_l}(l \to l')$ for $L_c = 0$.

6. Extension to Atoms with Hyperfine Structure

Experimental studies are focused on the evaluation of the excitation cross-sections without hyperfine structure. Excitation between two hyperfine levels is often overlooked and often unresolved experimentally. However, with modern observations, it has become possible to detect transitions between hyperfine levels, which implies the need for hyperfine collisional rates toward proper modeling. In fact, hyperfine levels are unresolved but can be inferred through experimental results by adopting suitable coupling. Let us consider an isotope of an atom with nuclear spin I and the total angular momentum of a hyperfine structure $F = J + I$. [35] provided a detailed discussion regarding the direct and indirect methods to calculate collisional hyperfine rates.

The indirect method is based on the frozen nuclear spin (FNS) approximation, which is convenient in stellar and solar contexts. This method is based on relating the (de)polarization rates of hyperfine levels to the (de)polarization rates of fine J-levels by a simple linear combination.

Our intention is to infer hyperfine collisional rates from the usual excitation rates C_{lu} given by the general formula given by Equation (4). This extension from C_{lu} to the hyperfine level rates $D^{k_F}(JIF \to J'I'F')$ can be performed in the framework of the FNS approximation, which was included first, by [36,37]:

$$D^{k_F}(JIF \to J'IF') = (2F+1)(2F'+1)\sum_k (2k+1) \times D^k(J \to J') \times \sum_{k_I}(2k_I+1) \begin{Bmatrix} J & I & F \\ J & I & F \\ k & k_I & k_F \end{Bmatrix} \begin{Bmatrix} J' & I & F' \\ J' & I & F' \\ k & k_I & k_F \end{Bmatrix} \tag{13}$$

If one replaces $D^k(J \rightarrow J')$ by its expression as a function of C_{ul} as given in the previous section, $D^{k_F}(JIF \rightarrow J'IF')$ can be retrieved by using C_{ul} values and the algebra coefficients given in Equation (13).

As an example, in the case of the D_2 line of the Na atom, the lower level is $3s\ ^2S_{\frac{1}{2}}$, and the upper level is $3p\ ^2P_{\frac{3}{2}}$. For the level $3s\ ^2S_{\frac{1}{2}}$, $J = 1/2$ and since the nuclear spin of the Na atom is $I = 3/2$, the hyperfine levels are given by $F = 1$ and 2. Similarly for the upper level, one finds that $F = |J - I|$,....,$J + I = 0$, 1, 2 and 3. These quantum number values should be included in Equation (13) to obtain the collisional excitation rates and the polarization transfer rates between hyperfine levels as linear combinations of the C_{lu} rates given in Equation (4). Thus, one can determine the excitation rates between hyperfine levels simply by knowing the C_{lu} values of our general law given by Equation (4).

7. Conclusions

Ref. [9] used the experimental and theoretical data available at that time to derive a general semi-empirical formula, which, due to its simplicity and generality, is currently one of the most widely employed formulae to obtain atomic excitation rates through collisions with electrons. In order to provide more recent, accurate and easy-to-use formulae, we presented a new formulation of the atomic excitation by impact with electrons based on the available experimental values of excitation cross-sections, which were validated by recent quantum cross-sections. We first obtained the excitation rates C_{lu} at a large range of temperatures for nine simple atoms via integration over the velocities of experimental cross-sections.

Secondly, we performed a generalized fit based on sophisticated GP numerical methods to obtain collisional excitation rates C_{lu} for any simple atom as a function of the temperatures and threshold energies, which characterizes the given atomic transitions. Then, we explained how simple/complex atom excitation and polarization transfer rates can be deduced from C_{lu} after suitable algebra transformations. Similarly, atoms with a hyperfine fine structure were also treated, and the collisional rates between hyperfine levels can be expressed as a function of C_{lu}. The results provided here may lead to important improvements in modeling spectral line formation in solar and stellar atmospheres.

Author Contributions: M.D. obtained the numerical results and wrote the original draft.; S.Q., F.M. and B.Z.A. have all contributed to the analysis, drafting, review and finalization of the submitted manuscript. All authors have read and agreed to the published version of the manuscript.

Funding: The Deanship of Scientific Research (DSR) at King Abdulaziz University (KAU), Jeddah, Saudi Arabia has funded this Project under grant no. (G: 033-130-1443).

Conflicts of Interest: The authors declare no conflict of interest.

References

1. Sahal-Bréchot, S.; Vogt, E.; Thoraval, S.; Diedhiou, I. Impact polarization of the Halpha line of hydrogen in solar flares: Calculations of electron and proton collisional anisotropic processes between the Zeeman excited sublevels. *Astron. Astrophys.* **1996**, *309*, 317.
2. Barklem, P.S. Accurate abundance analysis of late-type stars: Advances in atomic physics. *Astron. Astrophys. Rev.* **2016**, *24*, 1. [CrossRef]
3. Wang, K.; Bartschat, K.; Zatsarinny, O. Meléndez, J. Electron Scattering from Neutral Fe and Low-energy Photodetachment of Fe^-. *Astrophys. J.* **2018**, *867*, 63. [CrossRef]
4. Reggiani, H.; Amarsi, A.M.; Lind, K.; Barklem, P.S.; Zatsarinny, O.; Bartschat, K.; Fursa, D.V.; Bray, I.; Spina, L.; Meléndez, J. Non-LTE analysis of KI in late-type stars. *Astron. Astrophys.* **2018**, *627*, A177. [CrossRef]
5. Zatsarinny, O.; Bartschat, K.; Fernandez-Menchero, L.; Tayal, S.S. Photoionization of neutral iron from the ground and excited states. *Phys. Rev. A* **2019**, *99*, 023430. [CrossRef]
6. Bergemann, M.; Hoppe, R.; Semenova, E.; Carlsson, M.; Yakovleva, S.A.; Voronov, Y.V.; Bautista, M.; Nemer, A.; Belyaev, A.K.; Leenaarts, J.; et al. Solar oxygen abundance. *Mon. Not. R. Astron. Soc.* **2021**, *508*, 2236. [CrossRef]
7. Tayal, S.S.; Zatsarinny, O. Effective Collision Strengths and Radiative Parameters for Lines in the Sc ii Spectrum. *Astrophys. J. Suppl. Ser.* **2022**, *259*, 52. [CrossRef]
8. Seaton, M.J. The impact parameter method for electron excitation of optically allowed atomic transitions. *Proc. Phys. Soc.* **1962**, *79*, 1105. [CrossRef]

9. van Regemorter, H. Rate of Collisional Excitation in Stellar Atmospheres. *Astrophys. J.* **1962**, *136*, 906. [CrossRef]
10. Derouich, M.; Radi, A.; Barklem, P.S. Unified numerical model of collisional depolarization and broadening rates that are due to hydrogen atom collisions. *Astron. Astrophys.* **2015**, *584*, 64. [CrossRef]
11. Derouich, M. General model of depolarization and transfer of polarization of singly ionized atoms by collisions with hydrogen atoms. *New Astron.* **2017**, *51*, 32. [CrossRef]
12. Derouich, M. Comprehensive Data for Depolarization of the Second Solar Spectrum by Isotropic Collisions with Neutral Hydrogen. *Astrophys. J. Suppl. Ser.* **2020**, *247*, 72. [CrossRef]
13. Koza, J.R. *Genetic Programming: On the Programming of Computers by Means of Natural Selection*; The MIT Press: Cambridge, MA, USA, 1992.
14. Derouich, M.; Sahal-Bréchot, S.; Barklem, P.S. Collisional depolarization of the lines of complex atoms/ions by neutral hydrogen. *Astron. Astrophys.* **2005**, *434*, 779. [CrossRef]
15. Enemark, E.A.; Gallagher, A. Electron excitation of the sodium D lines. *Phys. Rev. A* **1972**, *6*, 192. [CrossRef]
16. Ehlers, V.; Gallagher, A. Electron excitation of the calcium 4227-Å resonance line. *Phys. Rev. A* **1973**, *7*, 1573. [CrossRef]
17. Leep, D.; Gallagher, A. Electron excitation of the lithium 6708-Å resonance line. *Phys. Rev. A* **1974**, *10*, 1082. [CrossRef]
18. Chen, S.T.; Leep, D.; Gallagher, A. Excitation of the Sr and Sr^+ resonance lines by electron impact on Sr atoms. *Phys. Rev. A* **1976**, *13*, 947. [CrossRef]
19. Chen, S.T.; Gallagher, A. Excitation of the Ba and Ba^+ resonance lines by electron impact on Ba atoms. *Phys. Rev. A* **1976**, *14*, 593. [CrossRef]
20. Leep, D.; Gallagher, A. Excitation of the Mg and Mg^+ resonance lines by electron impact on Mg atoms. *Phys. Rev. A* **1976**, *13*, 148. [CrossRef]
21. Chen, S.T.; Gallagher, A. Electron excitation of the resonance lines of the alkali-metal atoms. *Phys. Rev. A* **1978**, *17*, 551. [CrossRef]
22. Vriens, L.; Smeets, A.H.M. Cross-section and rate formulas for electron-impact ionization, excitation, deexcitation, and total depopulation of excited atoms. *Phys. Rev. A* **1980**, *22*, 940. [CrossRef]
23. Gao, X.; Han, X.Y.; Voky, L.; Feautrier, N.; Li, J.M. Precision calculation of low-energy electron-impact excitation cross sections of sodium. *Phys. Rev. A* **2010**, *81*, 022703. [CrossRef]
24. Lind, K.; Asplund, M.; Barklem, P.S.; Belyaev, A.K. Non-LTE calculations for neutral Na in late-type stars using improved atomic data. *Astron. Astrophys.* **2011**, *528*, A103. [CrossRef]
25. Lino, J.L.S. Cross sections for electron-impact excitation of neutral atoms. *Rev. Mex. Fis.* **2017**, *63*, 190.
26. Osorio, Y.; Barklem, P.S.; Lind, K.; Asplund, M. The influence of electron collisions on non-LTE Li line formation in stellar atmospheres. *Astron. Astrophys.* **2011**, *529*, A31. [CrossRef]
27. Amarsi, A.M.; Grevesse, N.; Grumer, J.; Asplund, M.; Barklem, P.S.; Collet, R. The 3D non-LTE solar nitrogen abundance from atomic lines. *Astron. Astrophys.* **2020**, *636*, A120. [CrossRef]
28. Sahal-Bréchot, S.; Derouich, M.; Bommier, V.; Barklem, P.S. Multipole rates for atomic polarization studies: The case of complex atoms in non-spherically symmetric states colliding with atomic hydrogen. *Astron. Astrophys.* **2007**, *465*, 667–677. [CrossRef]
29. Derouich, M.; Sahal-Bréchot, S.; Barklem, P.S. Spin depolarizing effect in collisions of simple/complex atoms in spherically symmetric states with neutral hydrogen. *Astron. Astrophys.* **2005**, *441*, 395–406. [CrossRef]
30. Barklem, P.S. Electron-impact excitation of neutral oxygen. *Astron. Astrophys.* **2007**, *462*, 781–788. [CrossRef]
31. Derouich, M.; Sahal-Bréchot, S.; Barklem, P.S. Collisional depolarization and transfer rates of spectral lines by atomic hydrogen-II. Application to d states of neutral atoms. *Astron. Astrophys.* **2003**, *409*, 369–373. [CrossRef]
32. Derouich, M. Étude des Collisions Dépolarisant les Raies du "Deuxième Spectre" du Soleil. Développement et Exploitation d'une Nouvelle Méthode Théorique. Ph.D. Thesis, Paris VII-Denis Diderot University, Paris, France, 2004. Available online: https://tel.archives-ouvertes.fr/tel-00331859 (accessed on 11 October 2022).
33. Derouich, M.; Barklem, P.S. Spin depolarizing effect in collisions with neutral hydrogen-II. Application to simple/complex ions in spherically symmetric states. *Astron. Astrophys.* **2007**, *462*, 1171–1177. [CrossRef]
34. Derouich, M. Collisional depolarization of molecular lines. Application to the SiO+H isotropic collisions. *Astron. Astrophys.* **2006**, *449*, 1–7. [CrossRef]
35. Derouich, M.; Basurah, H.; Badruddin, B. *Scattering Polarisation of the d-States of Ions and Solar Magnetic Field: Effects of Isotropic Collisions*; Cambridge University Press: Cambridge, UK, 2017; Volume 34, p. e018.
36. Nienhuis, G. Quantum-mechanical theory of transfer and relaxation of atomic multipole moments. *J. Phys. B Atom. Molec. Phys.* **1976**, *9*, 167. [CrossRef]
37. Omont, A. Irreducible components of the density matrix. Application to optical pumping. *Prog. Quantum Electron.* **1977**, *5*, 69–138. [CrossRef]